

# Structural and optical investigations of $TGB_A$ and $TGB_C$ mesophases exhibiting cylindrical and cone-like domain textures

A.C. Ribeiro<sup>1</sup>, L. Oswald<sup>2</sup>, J.F. Nicoud<sup>2</sup>, D. Guillon<sup>2,a</sup>, and Y. Galerne<sup>2</sup>

<sup>1</sup> Centro de Física da Matéria Condensada (U.L.), avenida Prof. Gama Pinto 2, 1699 Lisboa Codex, Portugal

<sup>2</sup> Institut de Physique et Chimie des Matériaux de Strasbourg, Groupe des Matériaux Organiques, 23 rue du Loess, 67037 Strasbourg Cedex, France

Received: 16 June 1997 / Revised: 17 October 1997 / Accepted: 20 November 1997

**Abstract.** The characterization by optical microscopy, X-ray diffraction and differential scanning calorimetry of two new liquid crystalline compounds is presented. The compounds under consideration incorporate in their molecules two chiral centres (one asymmetric carbon and one asymmetric sulphur of a sulphinate group). While the carbon chirality is fixed in the R configuration the sulphur chirality may be either in the S or in the R configuration. A  $TGB_A$  mesophase in a large temperature domain is evidenced for one of the two diastereomers, while both  $TGB_A$  and  $TGB_C$  mesophases are observed in a similar temperature domain for the other one. For both diastereomers and in both mesophases it is possible to observe the coexistence of two different types of optical textures, namely planar cholesteric textures and developable domains. The latter are coiled in a different way than proposed in an earlier publication. More precisely, they form cylindrical or cone-like domains with double-twist properties as observed in the blue phases. The pitch of the helix in the  $TGB$  mesophases is evaluated by means of optical reflection observations in samples exhibiting the planar cholesteric textures. For both diastereomers it is also possible to evaluate structural parameters related to the organization within the  $TGB_A$  mesophases. Finally, the induced phase transition  $TGB_C-S_C^*$  is studied by the application of an AC electric field.

**PACS.** 61.30.-v Liquid crystals

## 1 Introduction

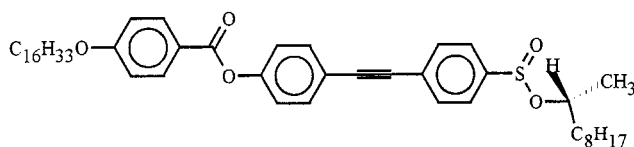
The analogy between the  $N-S_A$  phase transition and the transition between normal conductors and superconductors was established by de Gennes in 1972 [1]. The possible existence of a liquid crystalline phase similar to the Abrikosov phase present in type II superconductors lead Renn and Lubensky to predict in 1988 [2] the existence of a new frustrated smectic A phase called “twist grain boundary smectic A” or  $TGB_A$  phase. The latter could be observed in some cases with chiral molecules of liquid crystals, usually between the  $N^*$  and  $S_A$  phases. The model of molecular organization for this frustrated phase was also presented in reference [2]. In this frustrated smectic A phase where the distance between layers is  $d$ , there are blocks of smectic A layers arranged in an helical way along an axis parallel to the smectic blocks. Two adjacent smectic A blocks are rotated by an angle  $\alpha$  and they are separated by a grain boundary where exists a lattice of parallel and equidistant screw dislocation lines separated by a distance  $l_d$ . The distance between two adjacent grain boundaries is  $l_b$ . The angle between two families of adjacent screw dislocation lines belonging to adjacent

grain boundaries is  $\alpha = 2 \sin^{-1}(d/2l_d)$  (see Ref. [9]). The experimental evidence of the existence of such a phase was reported for the first time in 1989 by Goodby *et al.* [3]. But it is interesting to notice that all the details of a  $TGB_A$  mesophase were experimentally observed only in 1992 and confirmed by Ihn *et al.* [4] using freeze fracture electron micrographs. Meanwhile Lubensky and Renn [5] proposed some modifications to their initial description, namely to explain the existence of  $TGB_A$  mesophases in compounds not exhibiting the  $N^*$  mesophase. In addition, the possible existence of  $TGB_C$  and  $TGB_{C^*}$  mesophases was also predicted by Renn in 1991 [6] and the experimental evidence of the existence of such  $TGB_C$  mesophases has been demonstrated in 1992 by Nguyen *et al.* [7] in a series of new compounds. However, up to now, the  $TGB_{C^*}$  phase in which the smectic slabs have themselves an helical smectic structure is not discovered yet, and it may be very problematic to prove the existence of such a phase from the experimental point of view. The existence of integer commensurability in  $TGB_C$  mesophases, where the grain boundary angle  $\alpha$  is an integer ratio of  $2\pi$ , was reported for the first time in 1993 by Navailles *et al.* [8]. However, the origin of such a commensurability is so far unexplained, except for the trivial anchoring effect proposed recently [9].

<sup>a</sup> e-mail: guillon@michelangelo.u-strasbg.fr

In 1994 we reported for the first time the characterization of a mesogenic compound with two chiral centres exhibiting a  $TGB_A$  mesophase and showing simultaneously optical textures characteristic of columnar and cholesteric order [10]. To explain the columnar and cholesteric textures and the  $S_A$  behaviour as found by X-ray diffraction, we proposed a model of supramolecular organization in this phase [9, 10] that further experiments (see below in the text) revealed not to be consistent with the orientation of the molecules.

In this paper, two new compounds belonging to the same series as that exhibiting a large  $TGB_A$  range [10] are considered. Their molecules have exactly the same tolane core, the same aliphatic chain at one side of the molecule but a longer branched aliphatic chain connected to the sulphur chiral part. The chiral carbon centre is in the R configuration and both diastereomers with the chiral sulphur centre in the R and S configurations are studied.



One of the diastereomers presents a  $TGB_A$  mesophase in a wide temperature range, while the other one exhibits both  $TGB_A$  and  $TGB_C$  phases in a similar temperature domain. These phases are analyzed in detail with optical microscopy and X-ray diffraction investigations, together with electro-optical measurements under electric field and with the study of binary mixtures. We are thus led to modify the model of the developable domains proposed in reference [9].

## 2 Experimental

The synthesis of the diastereomers studied in this paper has been performed according to the method described elsewhere [11] for other terms of the same homologous series. The two pure diastereomers (R, R) and (S, R) have been separated by means of high pressure liquid chromatography. Both compounds were characterized by NMR, IR and elemental analysis and gave satisfactory data.

Powder X-ray diffraction patterns were recorded as a function of temperature using a Debye-Scherrer type camera with bent quartz monochromator ( $K\alpha_1$  radiation,  $\lambda = 1.54 \text{ \AA}$ ), an INSTEC hotstage ( $\pm 0.01 \text{ }^\circ\text{C}$ ) and an INEL curved position-sensitive gas detector associated with a data acquisition computer system. With this system it was possible to measure periodic distances up to  $60 \text{ \AA}$ , with an experimental resolution of  $\Delta 2\theta = 0.07^\circ$ . In order to investigate larger periodic distances, a vacuum small angle X-ray home built camera was used. It was equipped with a bent gold plated glass mirror (nickel filtered  $K\alpha$  copper radiation from a GX20 ELIOTT rotating anode X-ray generator), and an electric oven. In this case it was possible to measure periodic distances up to  $160 \text{ \AA}$  (the full width half maximum of the beam being  $\Delta 2\theta = 0.015^\circ$ ).

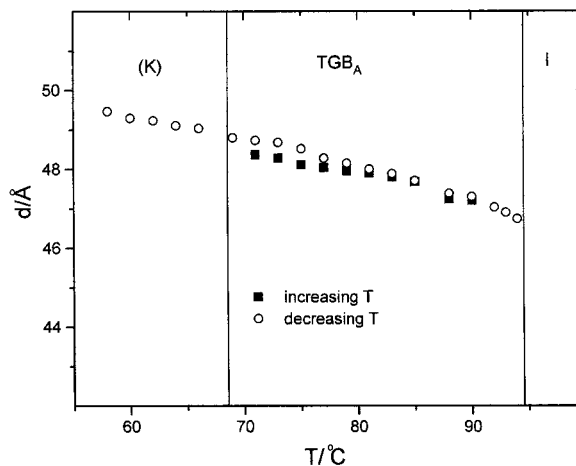


Fig. 1. Layer spacing as a function of temperature (diastereomer I). (K) corresponds to the supercooled state.

The diffraction patterns were registered on photographic films. In both setups, samples were housed in sealed Lindemann glass capillaries.

As for the optical microscopy, both transmission and reflective modes were used. The optical systems were associated with Mettler hot stages, temperature controlled. For the reflective observations the microscope was coupled with a spectrophotometer for visible light associated with a data acquisition computer system. In addition, for one of the compounds some electro-optical measurements have been performed to induce phase transitions by the effect of an AC electric field.

Differential scanning calorimetry measurements were performed using a Perkin-Elmer DSC7 apparatus.

## 3 Results

For both diastereomers studied in this paper, it was not possible till the moment to know exactly which one of them corresponds to sulphur chiral centre in R or S configuration. Therefore, hereafter we will refer to them as diastereomers I and II.

### 3.1 Diastereomer I

For the diastereomer I the existence of a mesophase was detected between the crystalline and the isotropic phases. As we shall see hereafter all the obtained results indicate that the mesophase under consideration is a  $TGB_A$  phase and that the compound has the following thermal behaviour:



The X-ray diffraction patterns registered with the Debye-Scherrer camera as a function of temperature are characteristic of a smectic A mesophase (Bragg sharp reflections in the small angle region and a diffuse signal

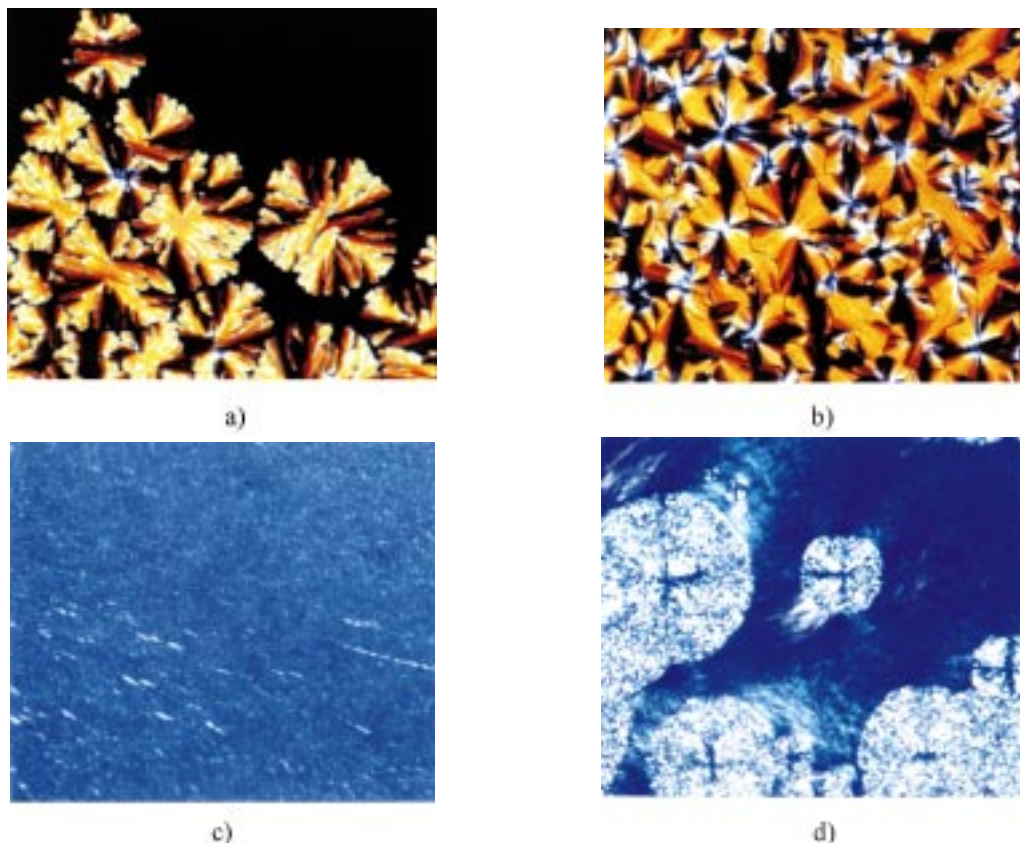


**Fig. 2.** Optical textures (magnification  $\times 210$ ) obtained with diastereomer I (transmission mode). a) Growing of developable units detected at  $T = 93.5$  °C on cooling very slowly from the isotropic phase. b) Developable units. This picture was observed in the  $TGB_A$  mesophase at  $T = 93$  °C. c) Planar cholesteric texture observed in the  $TGB_A$  at  $T = 72.2$  °C after a shear stress has been applied to a preparation similar to that shown in Figure 2b. d) Recrystallisation observed at  $T = 59.6$  °C.

in the wide angle region). For each temperature, the patterns were obtained on increasing and decreasing the temperature and registered at least during 30 minutes. The evolution of the layer spacing with temperature is displayed in Figure 1. The small decrease of the layer spacing with increasing temperature, in the mesophase, is mainly due to the increase of disorganization of the aliphatic chains. It is interesting to note the sharp profile of the Bragg peak, indicating the presence of a long-range smectic order in the TGB phase.

The optical microscopy observations show nice textures apparently associated with different kinds of structures. On cooling the sample very slowly from the isotropic phase, and using the polarizing microscope in the transmission mode, it was possible to observe the growing of a texture usually associated with the existence of columnar mesophases as shown in Figure 2a. In Figure 2b, obtained at  $T = 93$  °C, it is possible to observe clearly the existence of developable domains. The same type of texture was roughly preserved on cooling down to recrystallization. On the other hand, by applying a small pressure (cautiously exerted on the cover glass with a spatula) to a preparation similar to that shown in Figure 2b at the same temperature ( $T = 93$  °C), these textures are completely destroyed.

Moreover, any light transmission between crossed nicols could be detected then at this temperature. A bright blue color characteristic of interferences due to a cholesteric structure began to be visible at about  $T = 86$  °C, and then different tonalities of blue were observed on decreasing temperature till the recrystallization. For each temperature, no change of the colour in the transmitted light was detected on rotating the sample between crossed nicols. These observations are in agreement with the existence of an helical structure with the helical axis perpendicular to the plane of observation. Such a planar texture observed at  $T = 72.2$  °C in the mesophase is presented in Figure 2c whereas the occurrence of recrystallization at  $T = 59.6$  °C can be seen in Figure 2d.

The optical microscopy observations performed in the reflective mode, when pressure has been applied to the sample, showed that light at visible wavelengths was only reflected for temperatures lower than 86 °C. On decreasing temperature, different tonalities of blue were observed till the recrystallization, as observed in the transmission mode. Therefore, the evolution with temperature of the wavelengths of the maximum reflected light, detected with a spectrophotometer, was very smooth till the recrystallization. The corresponding temperature dependence of

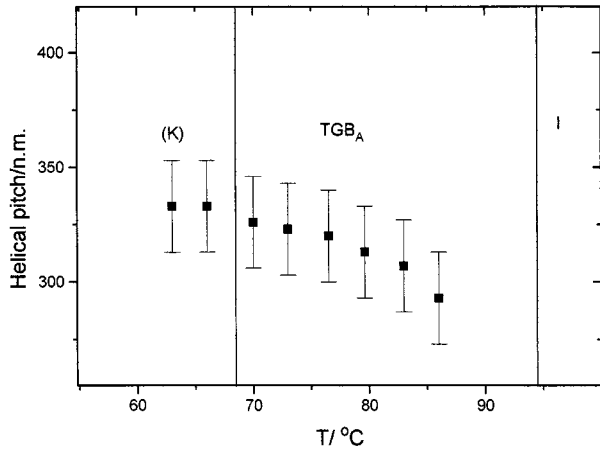


**Fig. 3.** Helical pitch as a function of temperature (diastereomer I). (K) corresponds to the supercooled state.

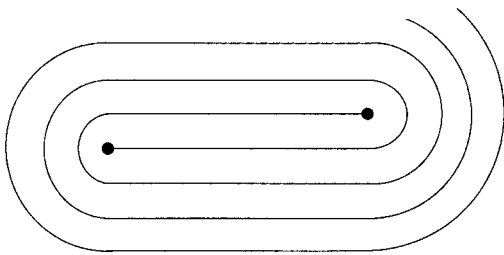


**Fig. 4.** Cylindrical domain. The solid lines sketch at the same time, the smectic blocks, the grain boundaries and the cholesteric layers. They moreover correspond to the projection direction of the molecules onto the plane of the figure, and in particular, they give the direction of the molecules when, during the helicoidal rotation, they come into this plane. The dots mark the axes of the cylinders; they correspond to the typical eyes of the cylindrical domains observed at the microscope.

the helical pitch of the twisted structure, estimated from the direct measurements of these wavelengths, is displayed in Figure 3 (the mean refraction index of the liquid crystal was assumed to be about 1.5).

All the above experimental observations on diastereomer I, namely the coexistence for the detected mesophase, of textures generally considered to be typical of columnar and cholesteric mesophases, and the X-ray patterns characteristic of a smectic A mesophase, suggest as for the compound described in reference [10] that this diastereomer exhibits a  $TGB_A$  mesophase in a large temperature range (26 °C). The apparent contradiction between the optical columnar and cholesteric textures and the lamellar nature of the phase can be understood with a model modified from the one presented in reference [9]. In fact, as further experiments have shown by means of a rotating compensator, the light waves which are polarized radially from the “eyes” of the developable domains [10], propagate with the smallest optical index. This indicates that the molecules are perpendicular to the radial directions. The smectic blocks, the grain boundaries and the layers of

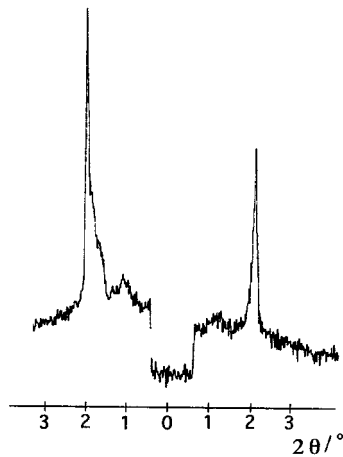
the helical structure of the TGB phase, are therefore coiled around the eyes of the domains as sketched with the solid lines in Figure 4, and not oriented radially as proposed in reference [9]. Such a structure is mechanically possible provided that the smectic blocks can be bent. Clearly, the bending of the smectic blocks in a plane perpendicular to the smectic layers is elastically disfavored since it needs compressions and dilations of the smectic layers, involving an energy density  $\frac{1}{2}B\left(\frac{\delta d}{d}\right)^2 \sim \frac{1}{2}Bl_b^2(\nabla\theta)^2$ , where  $d$  is the smectic layer thickness,  $B$  is the elastic constant for the uniaxial compressions,  $l_b$  is the thickness of the blocks and the angle  $\theta$  refers to the direction of the block normal. The block thickness  $l_b$  being of the order of a few molecular lengths,  $Bl_b^2$  is comparable to or one order of magnitude larger than the Frank elastic constant  $K$  and therefore, the compression energy involved in the bending of the smectic blocks just renormalizes their effective orientational elastic constants without preventing them to bend actually. In that sense, the TGB phases constitute layered systems which should build focal conics. However, the smectic blocks do not behave exactly as smectic layers. They cannot be elongated locally nor continuously in the direction perpendicular to their smectic layers, because the smectic layers themselves forbid any flow in that direction. They are therefore one dimensional liquids, with crystalline properties along the direction perpendicular to the smectic layers. This means in particular that the blocks have metric properties in this perpendicular direction which, due to helical twisting, extend to all the directions parallel to the block surface. This 2D metric condition prevents the blocks to be elongated in any manner. Therefore, like paper sheets, they cannot undergo bendings with double curvatures, as involved in the sphere for instance; in other words, they keep a zero Gaussian curvature whatever the deformations. Thus, the blocks can just be folded in cones and cylinders, the only surfaces which may be unrolled without elongations. The metric condition is then satisfied individually for each block, one block being possibly extended referred to the next one by introducing new smectic layers along all its length. The blocks are therefore able to slip against one another parallel to their neighbors, reducing the areas of the compression and dilation induced by the bends, to less than a block thickness  $l_b$ , as taken into account in the above calculation of the bending energy density. These systems, made of stacks of parallel planes, cylinders or cones (CC), may be seen as particular focal conics, since they are layered systems, but also as developable domains since they are particular developable domains which have their developable surfaces restricted to axes. Joined to the torus surfaces, they constitute a set which identifies to the intersection of both the sets of the focal conics and of the developable domains.

Figure 4 sketches a cylinder domain in a plane perpendicular to its axis, made of two cylinders connected by an undistorted region, consistent with the experimental observations [10]. It may be noticed that in such cylindrical domains, the smectic blocks are oriented according to the so-called double-twist, similarly as the

molecules in the blue phases. However, a remarkable feature here is that the double-twisted cylinders (proposed also by Kamien [12]), are able to extend over large distances, of the order of several hundred helical pitches, and so, their radius is not restricted to a quarter of a pitch as in the blue phases [13]. Naturally, the double-twisting applies to the whole TGB structure, and in particular, to the screw dislocations which are thus coiled helicoidally around the cylinder axes. With double-twisting, and if the splay-bend constant  $K_{24}$  is positive, the highly chiral phases realize a better minimization of the orientational elastic energy. The double-twist energy may be estimated to worth about  $-K$  per unit length of the cylinders, when taking the simple twisting of the cholesteric texture as a reference [13]; it is thus able to partially compensate the compression energies. The cylindrical configuration moreover, does not produce any defect in both the block and the helical orderings, nor along the connections between the three parts of Figure 4 for instance. Along the axes of the cylinders (Fig. 4), for symmetry reasons, the smectic layers should be oriented perpendicular to the direction of these axes, *i.e.* with the molecules parallel to the cylinder axes. In this way also, the cylindrical cores do not contain any compression energy, thus helping double-twisting to build up. So, the cylindrical domain organization globally appears to be energetically more favorable than the structure proposed in reference [9] where defects were anyhow necessary to break down both the block order and the cholesteric layering close to the cylinder axes.

The cone-like domains behave rather similarly as the cylindrical domains with a double-twisting of the whole structure, including the TGB dislocations. However, the cones need defects to build up. Along the axes, the orderings of the helical twisting, of the blocks and of the molecular orientations are destroyed. In particular, a disclination is necessary all along the cone axis, except where the molecules are parallel to it, which occurs marginally, for one block over  $N_b/2$ ,  $N_b$  being the number of blocks per helical pitch. The energetic cost of the complete cone-like domains could thus be heavy. Only parts of them could then build up, excluding the axis and its dislocation line. Such partial cone domains could nevertheless fill the whole space when stuck together in a polycrystalline array. Their aperture angle should not necessarily be small if the dislocation line along the cone axis is actually off the domain. In the opposite case, the aperture angle should keep smaller than  $l_b/D \sim 10^{-2}$  rd or 1 degree (with the block thickness  $l_b \sim 30$  nm, and the cell thickness  $D \sim$  a few micrometers) in order that the molecules can orient parallel to the axis all along it, allowing the dislocation to disappear.

It is interesting to point out that CC textures were always observed on cooling slowly from the isotropic phase in the absence of any orienting field. Most of the domains are incomplete and just correspond to a part of Figure 4. With their axis out of the domain, or rejected at the boundary to the neighbouring domains, they are probably of the cone-type for entropy reasons as evoked below, but this point cannot be ascertained experimentally. The



**Fig. 5.** X-ray profile, obtained with diastereomer I at  $T = 85^\circ\text{C}$ , in the region of very small diffraction angles.

CC textures form preferentially to the planar cholesteric textures (though exhibiting comparable elastic energies, if one takes double-twisting into account), essentially because they allow more possibilities, easier to adapt to uncontrolled anchoring conditions than the monocrystalline cholesteric textures. The larger versatility of the CC configurations arises from the numerous undetermined parameters that they offer, as the shape, the size and also the orientation of the domains. In particular, they have not really to be perpendicular to the cell plates though they look to be so under the microscope essentially because of the relatively thin cell thickness (a few  $\mu\text{m}$ ) compared to their size (several hundred  $\mu\text{m}$ ). The tilt angle of the cylinder or cone axes cannot be estimated therefore in our experiments, nor also the aperture angle of the cones. When a small pressure is applied onto the cell as described above, the resulting shear orients the smectic blocks parallel to the plates, and the helical axis perpendicular to them, subsequently destroying the CC domains. Thus, planar textures characteristic of the cholesteric organization are formed. It is interesting to emphasize that in the same preparation it is possible to observe the coexistence of both textures, planar and with CC domains, at any given temperature in the mesophase. This confirms that both textures have comparable energies.

Let us now consider the structural parameters of this TGB<sub>A</sub> phase. In previous experimental studies, the distance between the screw dislocation lines,  $l_d$ , has been found to be about 140-150 Å in a TGB<sub>A</sub> phase [4] and to vary between 96 and 120 Å in a TGB<sub>C</sub> phase [8]. In order to try to measure directly  $l_d$  for the TGB<sub>A</sub> phase of diastereomer I, small angle X-ray diffraction experiments were performed. The patterns were registered during at least 48 hours at four different temperatures. The relative positions of the diffracted signals were similar in all of them, and an example of such a pattern registered at  $T = 85^\circ\text{C}$  is presented in Figure 5 where the variation of intensity as a function of diffraction angle has been obtained from the photographic film using a microdensitometer. Two types of Bragg reflections were detected in the region of very small diffraction angles. First a sharp reflection which is clearly associated with the distance between the smectic layers and previously detected using

the Debye-Scherrer camera associated with a curved sensitive detector. Second, a broader, but nevertheless well defined reflection in a small angle region which could not be detected previously with the Debye-Scherrer camera (outside its range of detection). Due to its low intensity, this broad peak could not be fitted with confidence. Its position was determined at the maximum of intensity, with an error bar. The repetition distance associated with this reflection is thus  $(82.4 \pm 2.2)$  Å.

In fact, this distance can be attributed either to the distance,  $l_b$ , between smectic blocks, or to the distance,  $l_d$ , between dislocation lines. Let us consider the first case, *i.e.*  $l_b = 82.4$  Å. At  $85$  °C, the helical pitch is  $2975$  Å and  $N_b = (2975/82.4) \cong 36$ . The angle  $\alpha$  is then found to be about  $10^\circ$  and  $l_d$  close to  $274$  Å. This results in a ratio  $l_b/l_d \approx 0.3$ , which is smaller than the ratio predicted by Renn and Lubensky (about 1) and much smaller than the other values reported in the literature for  $TGB_A$  and  $TGB_C$  phases (between 1 and 13, the highest values corresponding generally to  $TGB_C$  phases). Therefore it seems reasonable to attribute the repetition distance associated with the broader reflection to the distance  $l_d$  between screw dislocation lines. This interpretation is in agreement with the model of Renn and Lubensky [2]. Indeed, the dislocation lines should correspond to regions where the volumic density is lower (no smectic order), and such an array of lines gives rise then to an X-ray diffraction peak, the width of which depends upon the coherence length. It is then possible to determine the main structural parameters of the  $TGB_A$  mesophase by taking into account the values of the layer spacing (Fig. 1) and of the helical pitch (Fig. 3) already measured as a function of temperature. At  $T = 85$  °C, the angle,  $\alpha$ , between adjacent smectic blocks is close to  $(33.7 \pm 1)^\circ$ ; the number,  $N_b$ , of blocks by helical pitch is close to  $(10.7 \pm 0.3)$ ; and the distance,  $l_b$ , between adjacent grain boundaries is close to  $(278 \pm 8)$  Å. The ratio  $l_b/l_d$  is then  $\approx 3.4$  similar to those already reported for other compounds. It has to be noticed that grain boundaries with a rectangular lattice of Scherk's surfaces, as evidenced in diblock copolymers [14], should not appear here because they need larger twist angles  $\alpha$ , close to  $90^\circ$ , than observed. Moreover, they should involve strong orientational distortions of too high elastic energy to be allowed in liquid crystal phases.

From the smooth temperature variation of the position of the small angle broad diffraction signal, it was possible to estimate the evolution of  $l_d$ ,  $\alpha$ ,  $N_b$  and  $l_b$  between  $89$  °C and  $73$  °C. The distance  $l_d$  between the screw dislocation lines shows a very small dependence with temperature (between  $(80.2 \pm 2.1)$  Å at  $73$  °C and  $(83.4 \pm 2.3)$  Å at  $89.2$  °C). The angle  $\alpha$  decreases very slowly with temperature from  $(35.2 \pm 1)^\circ$  at  $T = 73$  °C to  $(32.9 \pm 1)^\circ$  at  $T = 89.2$  °C, and as a consequence  $N_b$  increases slowly with temperature from  $(10.2 \pm 0.3)$  to  $(10.9 \pm 0.4)$  blocks between the same temperatures. Finally, the length  $l_b$  decreases with temperature from  $(317 \pm 9)$  Å at  $T = 73$  °C to a value smaller than  $(244 \pm 10)$  Å at  $T = 89.2$  °C (at this temperature no visible light was detectable by using the microscope in the reflective mode).

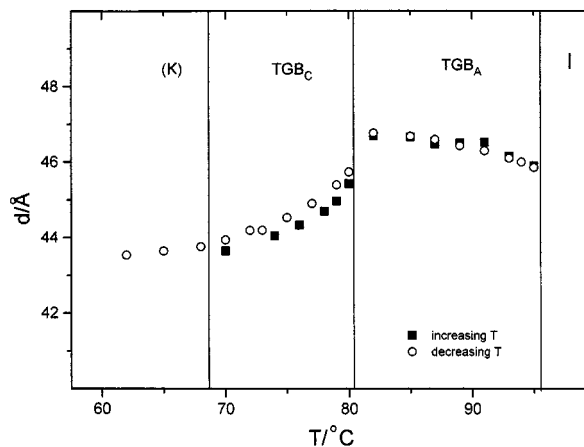
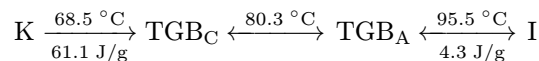


**Fig. 6.** Layer spacing as function of temperature (diastereomer II). (K) corresponds to the supercooled state.

## 3.2 Diastereomer II

### 3.2.1 Characterization

For the diastereomer II two mesophases between the crystalline and the isotropic phases were detected. As we shall see below all the experimental investigations indicate that the mesophases under consideration are of the  $TGB_A$  and  $TGB_C$  type. The thermal behaviour is thus the following:



the  $TGB_C$ – $TGB_A$  phase transition being of second order.

Powder X-ray diffraction patterns registered with the Debye-Scherrer camera as a function of temperature are typical of disordered smectic mesophases. As for the diastereomer I, the patterns were obtained on increasing and decreasing the temperature and registered at least during 30 minutes for each temperature. For both mesophases, the variation of the layer spacing with temperature is displayed in Figure 6. The increase of the layer spacing at low temperature and its slight decrease at higher temperature with increasing temperature are the signature of the smectic C and A phases.

The observations performed with the polarizing microscope in the transmission mode were similar to those obtained with diastereomer I exhibiting the  $TGB_A$  mesophase. In fact, on cooling very slowly from the isotropic phase it was possible to detect the formation of CC domains in the  $TGB_A$  phase as shown in Figure 7a. In the  $TGB_C$  phase a similar texture made of CC domains with some fracture lines as shown in Figure 7b was observed. They are probably due to uniaxial stresses which result from the changes with temperature in the characteristic distances,  $l_b$  or  $(2\pi l_b/\alpha)$  the pitch of the helical structure. When looking carefully at a CC domain, one observed two types of lines, both parallel to the solid lines in Figure 4. The most numerous lines appear very tiny first and get more and more visible on decreasing temperature, while

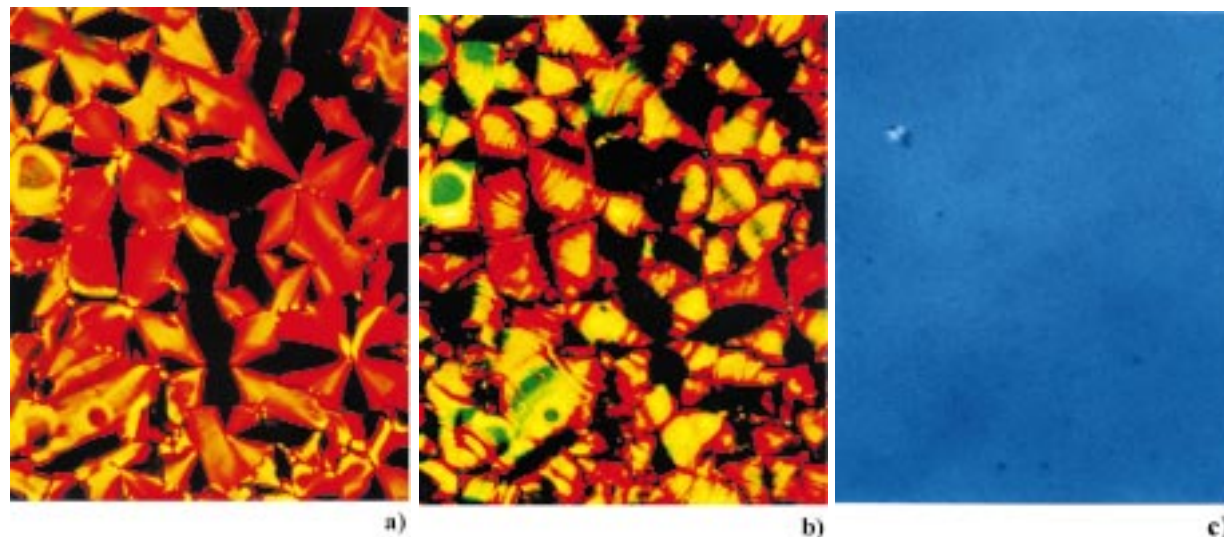


**Fig. 7.** Optical textures (magnification  $\times 210$ ) observed with diastereomer II. a) CC domains detected in the  $TGB_A$  mesophase at  $T = 93.9$  °C on decreasing the temperature very slowly from the isotropic phase. b) CC domain detected in the  $TGB_C$  mesophase at  $T = 77.4$  °C in the same region of picture 7a. c) Blue cholesteric planar texture obtained at  $T = 93.9$  °C when a slight pressure is applied to a sample similar to (7a) in the  $TGB_A$  mesophase.

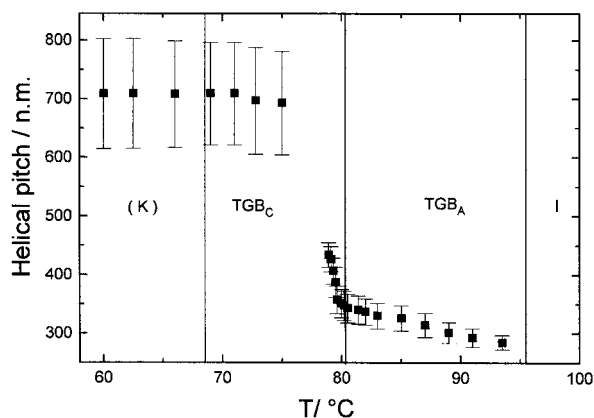


**Fig. 8.** Helical pitch as a function of temperature (diastereomer II). (K) corresponds to the supercooled state.

the second type of lines seem to be drawn with a pen in a definite point which goes ahead as the temperature is decreased. This moving point seems to correspond to a  $\chi$  line (edge dislocation line in the cholesteric ordering, or unwinding line) roughly perpendicular to the preparation. This  $\chi$  line changes the number of the cholesteric layers inside the CC domain. The whole texture with the CC domains is thus globally preserved till recrystallization.

As for diastereomer I the texture shown in Figure 7a was easily destroyed by applying a small pressure on the preparation. However, for diastereomer II, using the transmission mode in optical microscopy, a blue homogeneous cholesteric texture began to appear just below the transition to the isotropic phase as shown in Figure 7c. On decreasing further the temperature within the  $TGB_A$  phase, the texture remained practically the same with different tonalities of blue in a large temperature domain as for the

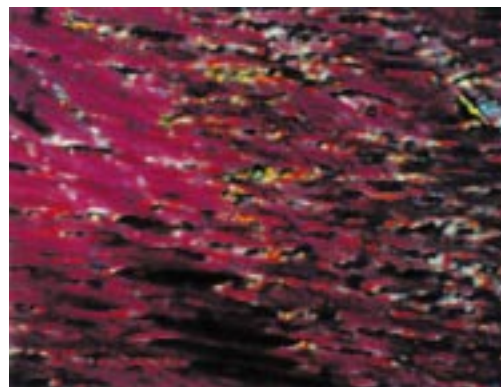


**Fig. 9.** Bookshelf texture (magnification  $\times 210$ ) observed at  $T = 77$  °C in a SSFLC cell of the  $S_C^*$  induced mesophase.

diastereomer I. At the transition between the two TGB mesophases the color of the texture varies towards a grey-blue one and does not change any more till the recrystallization.

By using optical microscopy in the reflective mode after applying a small pressure as described above, visible wavelengths were detected at temperatures lower than 94 °C. Different tonalities of bright blue color in cholesteric planar textures were observed in the  $TGB_A$  mesophase, and a green reflected light appeared when approaching the  $TGB_C$  mesophase. On crossing the transition temperature between the two mesophases, a rapid transformation of the green light into a red one occurred within a temperature range of 1.6 °C. By decreasing further the temperature into the  $TGB_C$  mesophase, second order reflections were detectable. For these reflections no variation of the reflected light color was observed with temperature till recrystallization. The variation of the helical pitch

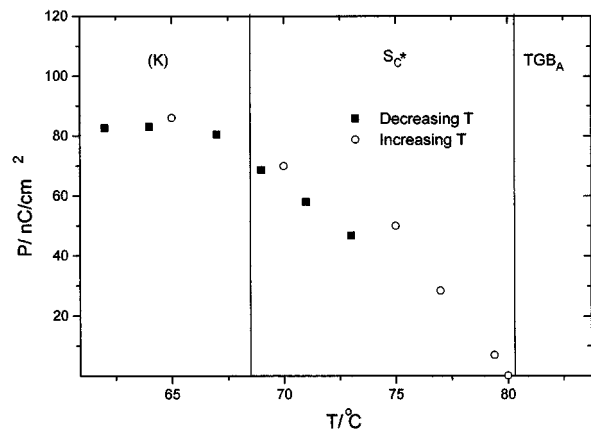


**Fig. 10.** Spontaneous polarization as a function of temperature in the  $S_{C^*}$  induced phase. (K) corresponds to the super-cooled state.



**Fig. 11.** Fan-broken texture (magnification  $\times 210$ ) detected in the induced  $S_{C^*}$  at  $T = 73^\circ\text{C}$ .

associated with the  $TGB_A$  and  $TGB_C$  structures, estimated from the direct measurements of the wavelengths of the maximum reflected light, is displayed in Figure 8 as a function of temperature. From the comparison of Figures 3 and 8 it is possible to conclude that the variation of the helical pitch with temperature is similar in the  $TGB_A$  mesophases of both diastereomers. However with diastereomer II the helical pitch increases strongly at the transition between the  $TGB_A$  and  $TGB_C$  mesophases as reported recently [15]. This behaviour has also been confirmed by other helical pitch measurements performed on diastereomer II using the thin wedge technique [16]. Then, in the  $TGB_C$  mesophase the helical pitch does not seem to change in a large temperature domain (till the recrystallization).

All the above experimental observations performed on diastereomer II confirm that this compound exhibits  $TGB_A$  and  $TGB_C$  mesophases in temperature ranges of  $15.2^\circ\text{C}$  and  $11.8^\circ\text{C}$  respectively.

As for diastereomer I, additional X-ray diffraction investigations have been performed on diastereomer II by using the home-built X-ray camera, in order to observe the reflections at very small diffraction angles correspond-

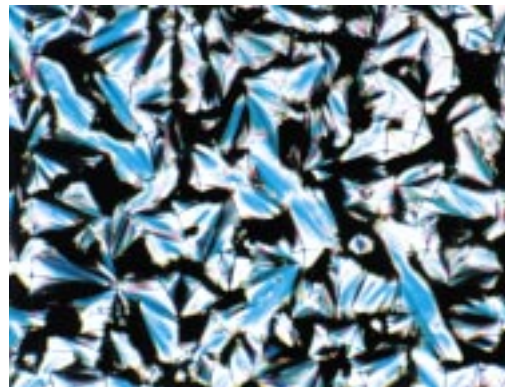


**Fig. 12.** Focal conics texture (magnification  $\times 210$ ) obtained on mixing I and II in equal percentages detected at  $T = 94.7^\circ\text{C}$ .

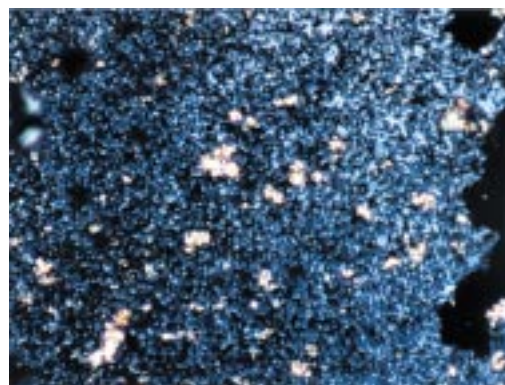


**Fig. 13.** Schlieren texture (magnification  $\times 210$ ) observed in the  $S_{C^*}$  phase of a mixture in equal percentages of I and II ( $T = 68^\circ\text{C}$ ). The glasses were treated with silane.

ing to the screw dislocation lattice of its  $TGB$  mesophases. Unfortunately in the case of diastereomer II, these investigations were made difficult since this compound showed a strong tendency to degradation when heated for long periods of time. However, it was possible to obtain one pattern in the  $TGB_A$  mesophase at  $T = 89^\circ\text{C}$  with an exposure time of 20 hours. The pattern was not so clear as those obtained with diastereomer I but it was possible to conclude that its intensity profile was similar to that one presented in Figure 5 obtained with diastereomer I. From the position of the broad reflection detected in the small angle region it was possible to estimate  $l_d$  close to  $(78.3 \pm 3) \text{ \AA}$  for a layer thickness of  $46.5 \text{ \AA}$ . In this way, the angle  $\alpha$  between smectic blocks should be close to  $(34.6 \pm 1.3)^\circ$ , the number of blocks by helical pitch  $N_b$  about  $(10.4 \pm 0.4)$  and the distance  $l_b$  between adjacent grain boundaries close to  $(290 \pm 11) \text{ \AA}$ . It was not possible to register other patterns for other temperatures in this  $TGB_A$  mesophase due to the small amount of compound available, and due to the tendency to degradation mentioned above. It was not possible also to have additional information about the  $TGB_C$  mesophase by means of small angle X-ray diffraction patterns.



### 3.2.2 TGB<sub>C</sub> – S<sub>C\*</sub> phase transition induced by an electric field

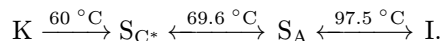
The TGB<sub>C</sub>–S<sub>C\*</sub> phase transition was induced under the effect of an electric field. The compound was introduced in the isotropic phase between two conducting glasses treated with Teflon in a 6 μm thickness cell. The sample was observed with a polarizing microscope in the transmission mode. On cooling from the isotropic phase, planar cholesteric textures similar to those previously described are obtained in the TGB<sub>A</sub> temperature range. At  $T = 73\text{ °C}$  in the TGB<sub>C</sub> mesophase the sample was submitted to an electric triangular field (40V p.p., 70 Hz) and the planar cholesteric texture was destroyed. The effect of the electric field was to drive the occurrence of a bookshelf organization similar to that usually detected in the SSFLC cells [17,18] of S<sub>C\*</sub> ferroelectric liquid crystals as shown in Figure 9. The variation as a function of temperature of the electric polarization measured in the S<sub>C\*</sub> induced mesophase is shown in Figure 10. Let us note that the accuracy of the data close to the transition is not sufficient to observe the classical parabolic behaviour for a second order transition. CC domains in very small areas of the cell were also present close to the borders of the preparation in the TGB<sub>A</sub> mesophase. When in the TGB<sub>C</sub> mesophase, the electric field drives the formation of fan-broken textures in these regions, as shown in Figure 11. These textures are indeed characteristic of a S<sub>C\*</sub> mesophase. The electro-optical experiments described above show clearly that diastereomer II exhibits a TGB<sub>C</sub> mesophase.

### 3.3 Mixture of diastereomers I and II

The TGB mesophases disappear on mixing diastereomers I and II in equal percentage. By observing a sample of this kind of mixture with the polarizing microscope in the transmission mode and on cooling it from the isotropic phase, a transition to a mesophase was detected at  $T = 97.5\text{ °C}$ . This mesophase was characterized by a focal conic texture, characteristic of a disordered smectic, as shown in Figure 12. Small pressure applied on the preparation was only able to change the dimensions of the focal conics which became smaller but always present. After some time of relaxation the focal conics become well developed again and a texture similar to that represented in Figure 12 could be observed. Decreasing even more the temperature does not change the general aspect of the texture till 69 °C. Around this temperature, some well developed fan-broken textures appeared.

In order to better understand the mesomorphic behaviour of this mixture, some supplementary microscopy observations were carried out using surface treated glasses with silane. Once again, on decreasing the temperature from the isotropic phase the same phase transitions were detected. Below  $T = 97.5\text{ °C}$ , large homeotropic areas were detected now in the high temperature mesophase and this result shows, as expected, that the mesophase under consideration is of the smectic A type. Further cooling led to the observation of a phase transition at  $T = 69.6\text{ °C}$ . In

the regions where the preparation appeared homeotropic at higher temperatures, a small transmission of light was detectable and schlieren textures characteristic of a S<sub>C\*</sub> mesophase as shown in Figure 13 were observed. The thermal behaviour of the mixture is the following:



As a final remark, it is important to note that with such a mixture, it was not possible to observe in any case the existence of CC domains.

In summary, it is possible to conclude that on mixing both diastereomers in equal percentage the TGB character disappears. In such a mixture one can consider that the chiral effect of molecules I and II with opposite configurations at sulphur roughly compensates. Since the similar compounds, containing a sulphinate group as the unique centre of chirality [19] do not exhibit any TGB phase, the TGB behaviour observed for the compounds in the present work is most probably due to a cooperative effect between the two chiral centres, which significantly enhances the molecular chirality.

## 4 Conclusion

The compounds studied in this paper exhibit TGB<sub>A</sub> and TGB<sub>C</sub> mesophases in large temperature domains. It is worthwhile to stress this feature since generally the existence of these phases was detected in smaller temperature ranges for other compounds described in literature. In the case of both compounds studied here, the values of the angle  $\alpha$  (35°) and of the distance  $l_b$  (about 300 Å) between two successive smectic blocks are similar to those found by Navailles in the case of a TGB<sub>C</sub> phase in another compound [20]. However it is worth mentioning also that the angle  $\alpha$  is practically the double of the angle detected with the compounds studied in references [4,8] while the dimension  $l_b$  is similar to that one reported for the compound studied in [4], but significantly smaller than the values reported in [8].

The results presented in this work and in particular the variation of  $N_b$  as a function of temperature (see Fig. 14) seem to indicate that the TGB<sub>A</sub> mesophase of diastereomer I exhibits an incommensurate behaviour of integer order as previously observed for other compounds [4], with however possible intermittencies (Fig. 14). For diastereomer II, an incommensurate behaviour is also observed at  $T = 85\text{ °C}$ , but the extension of such a behaviour in the whole temperature range of the TGB<sub>A</sub> phase cannot be precised. As for the TGB<sub>C</sub> mesophase detected in diastereomer II, it was not possible to conclude about the commensurability or incommensurability of this phase. Further work using two-dimensional X-ray diffraction on oriented samples [8] of different thickness will be very useful to clarify this point.

The most important conclusion of this paper is associated with a new interpretation of the optical textures observed in the TGB phases involving cylindrical and cone-like domains. The latter are in fact particular developable

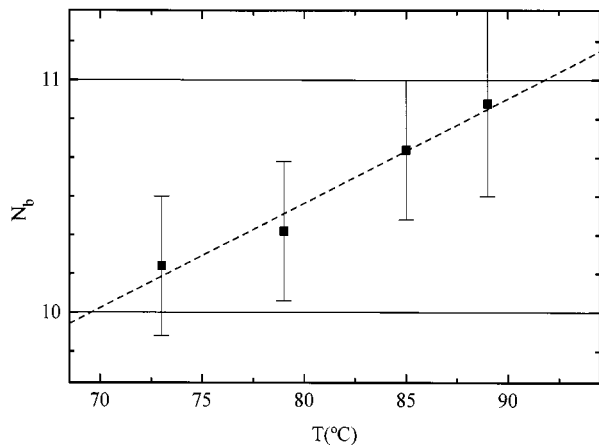


**Fig. 14.** Number of blocks  $N_b$  by helical pitch as a function of temperature in the TGB<sub>A</sub> mesophase of diastereomer I. The dashed line is a guide for the eye.

domains which were at the origin of the previous model proposed to explain the optical textures. The interpretation presented here is in agreement with all the experimental observations including the optical determination of the molecular directions, and is quite satisfactory from the energetic point of view essentially because of the double-twisting energy gain. Presumably, this model should also be applied to the TGB phases of any compound.

A.C. Ribeiro wishes to thank Dr Nguyen Huu Tinh (CRPP-Bordeaux) for helpful comments and suggestions, Dr Helena Godinho (FCT-UNL - Lisboa) for the use of the reflection microscope, and Praxis XXI (project 3/3-1/MMA/1769/95) for financial support.

## References

1. P.G. de Gennes, *Solid State Commun.* **10**, 753 (1972).
2. S.R. Renn, T.C. Lubensky, *Phys. Rev. A* **38**, 2132 (1988).
3. J.W. Goodby, M.A. Waugh, S.M. Stein, E. Chin, R. Pindak, J.S. Patel, *Nature (London)* **337**, 449 (1989); *J. Am. Chem. Soc.* **111**, 8119 (1989).
4. K.J. Ihn, J.A. Zasadzinski, R. Pindak, A.J. Slaney, J. Goddby, *Science* **258**, 275 (1992).
5. T.C. Lubensky, S.R. Renn, *Phys. Rev. A* **41**, 4392 (1990).
6. S.R. Renn, *Phys. Rev. A* **45**, 953 (1992).
7. H.T. Nguyen, A. Bouchta, L. Navailles, P. Barois, N. Isaert, R.J. Twieg, A. Maaroufi, C. Destrade, *J. Phys. II France* **2**, 1889 (1992).
8. L. Navailles, P. Barois, H.T. Nguyen, *Phys. Rev. Lett.* **71**, 545 (1993).
9. Y. Galerne, *J. Phys. II France* **4**, 1699 (1994).
10. A.C. Ribeiro, A. Dreyer, L. Oswald, J.F. Nicoud, A. Soldera, D. Guillon, Y. Galerne, *J. Phys. II France* **4**, 407 (1994).
11. a) A. Soldera, J.F. Nicoud, Y. Galerne, A. Skoulios, D. Guillon, *Liq. Cryst.* **12**, 347 (1992); b) A. Soldera, J.F. Nicoud, A. Skoulios, Y. Galerne, D. Guillon, *Chem. Mater.* **6**, 625 (1994).
12. R.D. Kamien, *J. Phys. II France* **7**, 743 (1997).
13. P.G. de Gennes, J. Prost, *The Physics of Liquid Crystals*, 2<sup>nd</sup> edition (Clarendon Press Oxford, 1993).
14. S.P. Gido, J. Gunther, E.L. Thomas, D. Hoffman, *Macromol.* **26**, 4506 (1993).
15. N. Isaert, L. Navailles, P. Barois, H.T. Nguyen, *J. Phys. II France* **4**, 1501 (1994).
16. N. Isaert, private communication.
17. N. Clark, S. Lagerwall, *Appl. Phys. Lett.* **36**, 899 (1980).
18. R. Shao, J. Pang, N. Clark, J.A. Rego, D.M. Walba, *Ferroelectrics* **147**, 255 (1993).
19. M.Z. Cherkaoui, J.F. Nicoud, D. Guillon, *Chem. Mat.* **6**, 2026 (1994).
20. L. Navailles, Thesis University Bordeaux I (1994).